

Nonthermal Emission Associated with Strong AGN Outbursts at the Centers of Galaxy Clusters

Yutaka Fujita¹, Kazunori Kohri^{2,3}, Ryo Yamazaki⁴, and Motoki Kino^{1,5}

ABSTRACT

Recently, strong AGN outbursts at the centers of galaxy clusters have been found. Using a simple model, we study particle acceleration around a shock excited by an outburst and estimate nonthermal emission from the accelerated particles. We show that emission from secondary electrons is consistent with the radio observations of the minihalo in the Perseus cluster, if there was a strong AGN outburst $\gtrsim 10^8$ yrs ago with an energy of $\sim 1.8 \times 10^{62}$ erg. The validity of our model depends on the frequency of the large outbursts. We also estimate gamma-ray emission from the accelerated particles and show that it could be detected with *GLAST*.

Subject headings: acceleration of particles — radiation mechanisms: non-thermal — galaxies: active — galaxies: clusters: general — galaxies: clusters: individual: Perseus (A426)

1. Introduction

Diffuse synchrotron radio emission is often found in the intracluster medium (ICM) of galaxy clusters (e.g., Kim et al. 1990; Giovannini et al. 1993; Giovannini & Feretti 2000; Kempner & Sarazin 2001). These radio sources in clusters are often classified as either

¹Department of Earth and Space Science, Graduate School of Science, Osaka University, 1-1 Machikaneyama-cho, Toyonaka, Osaka 560-0043, Japan; fujita@vega.ess.sci.osaka-u.ac.jp

²Institute for Theory and Computation, Harvard-Smithsonian Center for Astrophysics, MS-51, 60 Garden Street, Cambridge, MA 02138

³Physics Department, Lancaster University, Lancaster LA1 4YB, UK; k.kohri@lancaster.ac.uk

⁴Department of Physics, Hiroshima University, Higashi-Hiroshima, Hiroshima 739-8526, Japan; ryo@theo.phys.sci.hiroshima-u.ac.jp

⁵Institute of Space and Astronautical Science, JAXA, 3-1-1 Yoshinodai, Sagamihara, Kanagawa 229-8510, Japan; kino@vsop.isas.jaxa.jp

peripheral cluster radio relic sources or central cluster radio halo sources. Since most of the relics and halos are found in merging clusters, the particles responsible for the emission are thought to be accelerated at shocks or turbulence excited by cluster mergers (Roettiger et al. 1999; Takizawa & Naito 2000; Fujita & Sarazin 2001; Brunetti et al. 2001; Ohno, Takizawa, & Shibata 2002; Fujita, Takizawa, & Sarazin 2003; Brunetti et al. 2004).

However, there are exceptional diffuse radio sources. They are called ‘minihalos’ and are located in the central regions of non-merging clusters or ‘cooling core’ clusters (Baum & O’Dea 1991; Burns et al. 1992; Rizza et al. 2000). Gitti et al. (2002) suggested that the diffuse synchrotron emission from radio minihalos is due to a relic population of relativistic electrons reaccelerated by MHD turbulence via second-order Fermi acceleration, and that the energy is supplied by cooling flows. Alternatively, Pfrommer & Enßlin (2004) discussed that the electrons responsible for the synchrotron emission from minihalos are of secondary origin and thus are injected during proton-proton collision in the ICM. However, Gitti et al. (2002) did not discuss the generation of the turbulence, and Pfrommer & Enßlin (2004) did not investigate the mechanism of proton acceleration.

Recent X-ray observations have shown that AGNs at the centers of galaxy clusters sometimes exhibit intensive outbursts with a mechanical power of $\sim 10^{61}$ erg. The examples are MS 0735.6+7421 (McNamara et al. 2005; Gitti et al. 2007), Hercules A (Nulsen et al. 2005a), and Hydra-A (Nulsen et al. 2005b; Wise et al. 2007). Such an intensive outburst should excite a shock in the ICM. In fact, weak shocks have been found in those clusters. In the early stage of the evolution of the shock, the Mach number is expected to be large. Therefore, particles would be accelerated at the shock as in the case of a supernova remnant.

In this letter, we consider particle acceleration at the shock generated by an intensive outburst of the AGN at the cluster center. We study nonthermal emission from the accelerated particles. In particular, we focus on nonthermal radio emission of secondary origin. Recently, Hinton & Domainko (2007) estimated gamma-ray emission associated with AGN outbursts, assuming that the hot cavity behind a shock is entirely filled with high-energy protons. This assumption may be too simple, and they did not discuss the acceleration and energy spectrum of protons. However, motivated by this study, we also estimate the gamma-ray emission using our model. We take the Perseus cluster as a model cluster, because this cluster has a well-studied minihalo.

2. Models

We assume that the duration of an AGN outburst is $\sim 10^7$ yr. Since we are interested in the evolution of a shock for $t \gtrsim 10^7$ yr, where $t = 0$ corresponds to the ignition of the outburst, the evolution can be approximated by that of an instant explosion with an energy of E_0 at $t = 0$.

For the sake of simplicity, we assume that the cluster is spherically symmetric and the density profile of the ICM has a form of a power-law:

$$\rho_{\text{ICM}}(r) = \rho_1(r/r_1)^{-\omega}. \quad (1)$$

We take $\rho_1 = 5.3 \times 10^{-25} \text{ g cm}^{-3}$, $r_1 = 10 \text{ kpc}$, and $\omega = 1.43$, based on the density profile of the Perseus cluster for $70 < r < 300 \text{ kpc}$ (Fig. 8 in Churazov et al. 2003). We take that region because our model is correct for $t \gtrsim 1 \times 10^7$ yr, and the radius of the shock at $t \sim 10^7$ yr is $R_s \sim 70 \text{ kpc}$ for parameters we adopt in §3.

Using a shell approximation (e.g. Ostriker & McKee 1988), the radius of the shock can be written as

$$R_s = \xi \left(\frac{E_0}{\rho_1 r_1^\omega} \right)^{1/(5-\omega)} t^{2/(5-\omega)}, \quad (2)$$

where

$$\xi = \left[\left(\frac{5-\omega}{2} \right)^2 \frac{3}{4\pi} \frac{(\gamma+1)^2(\gamma-1)(3-\omega)}{9\gamma-3-\omega(\gamma+1)} \right]^{1/(5-\omega)}, \quad (3)$$

and $\gamma (= 5/3)$ is the adiabatic index. The Mach number of the shock gradually decreases. The shock stops expanding when its Mach number approaches to one. At this point, the cavity filled with hot gas inside the shock becomes in pressure equilibrium with the surrounding ICM. Since we stop calculation before the radiative cooling of the shock becomes effective ($\gtrsim \text{Gyr}$), we do not need to consider the radiative cooling.

Following Yamazaki et al. (2006), we assume that particles are accelerated at the shock via diffusive shock acceleration (i.e., first-order Fermi acceleration) and that their energy spectra are given by

$$N(E) \propto E^{-x} e^{-E/E_{\text{max}}}, \quad (4)$$

where E_{max} is the maximum energy of the protons or electrons. The index is given by $x = (r_b + 2)/(r_b - 1)$, where r_b is the compression ratio of the shock (Blandford & Eichler 1987). We estimate the maximum energies of the protons and electrons using the relations of

$$t_{\text{acc}} = \min\{t_{pp}, t\}, \quad t_{\text{acc}} = \min\{t_{\text{syn}}, t\}, \quad (5)$$

respectively. Here, t_{acc} , t_{pp} , t and t_{syn} are the acceleration time, the lifetime of high-energy protons through pion production, the age of the shock wave, and the synchrotron cooling time, respectively.

Assuming the standard manner for the diffusion coefficient, the acceleration time is given by

$$t_{acc} = \frac{20hcE_{\max}}{eB_dV_s^2}, \quad (6)$$

where c is the speed of light, $-e$ is the electron charge, and $V_s(= dR_s/dt)$ is the shock velocity (Jokipii 1987; Yamazaki et al. 2004). The correction factor h depends on the mean free path of particles and the angle between the shock and the magnetic field. Since $h \sim 1$ in the Bohm-limit case, we assume that $h = 1$ from now on. The downstream magnetic field is given by $B_d = r_b B$, where B is the magnetic field strength of the unperturbed ICM. We estimate t_{pp} as

$$t_{pp} = 5.3 \times 10^7 \text{ yr } (n_{\text{ICM}}/\text{cm}^{-3})^{-1}, \quad (7)$$

where n_{ICM} is the number density of the ICM. Since the shock is in pressure equilibrium in $\sim 10^8$ yr (see §3) and $n_{\text{ICM}} \lesssim 0.1 \text{ cm}^{-3}$, the cooling is not effective. Thus, the maximum energy of protons is determined by the age of the shock. On the other hand, the synchrotron cooling time for electrons is given by

$$t_{syn} = 1.25 \times 10^4 \text{ yr } \left(\frac{E_{\max,e}}{10 \text{ TeV}} \right)^{-1} \left(\frac{B_d}{10 \mu \text{ G}} \right)^{-2}, \quad (8)$$

and is shorter than the age of the shock. Thus, using relations (5), we obtain

$$E_{\max,p} \sim 1.6 \times 10^2 \left(\frac{V_s}{10^3 \text{ km s}^{-1}} \right)^2 \left(\frac{B_d}{10 \mu \text{ G}} \right) \left(\frac{t}{10^5 \text{ yr}} \right) \text{ TeV}, \quad (9)$$

$$E_{\max,e} \sim 14 \left(\frac{V_s}{10^3 \text{ km s}^{-1}} \right) \left(\frac{B_d}{10 \mu \text{ G}} \right)^{-1/2} \text{ TeV}. \quad (10)$$

We assume that the minimum electron and proton energies are their rest masses. For given proton and electron spectra, we calculate radiation from them. We consider the synchrotron, bremsstrahlung, and inverse Compton emissions from primary electrons that are directly accelerated at the shock, the π^0 -decay gamma-ray through proton-proton collisions, and the synchrotron, bremsstrahlung, and inverse Compton emissions from secondary electrons created through the decay of charged pions that are also generated through proton-proton collisions (Sturmer et al. 1997; Kohri, Yamazaki, & Bamba 2007). The density of target protons for the proton-proton interaction is given by $r_b \rho_{\text{ICM}}(R_s)/(1.4 m_p)$, where m_p is the proton mass. We assume that the spectrum from secondary electrons is stationary

if the lifetime of the electrons is smaller than the age of the system. On the other hand, if the lifetime is larger than the system age, we calculate the evolution according to §3 of Atoyan & Aharonian (1999) (see also Kohri et al. 2007).

3. Results

In our model, the evolution of a shock is determined by ρ_{ICM} and E_0 (equation [2]). The Mach number also depends on the ICM temperature, T . The energy spectrum of particles depends on the evolution of the shock and the magnetic field, B . The luminosity of nonthermal emission from the shock depends on the total energy of high-energy ($> m_p c^2$) protons inside the shock, ϵE_0 , where $0 \leq \epsilon \leq 1$. We fix $\rho_{\text{ICM}}(r)$, T , and $B(r)$ from observations. On the other hand, we regard E_0 and ϵ as fitting parameters, because there are no observational data for them.

We assume that $T = 3.5$ keV, which is the temperature of the central region of the Perseus cluster (Churazov et al. 2003), although the temperature before the outburst might have been somewhat lower. As far as we know, there are no observations of magnetic fields in the Perseus cluster at $r \gtrsim 70$ kpc. On the other hand, the observations of Faraday rotation showed that the typical magnetic field strength in clusters for $r \lesssim 500$ kpc is 5–10 μG (Clarke, Kronberg, & Böhringer 2001). Therefore, we take $B(r) = 7\mu\text{G} (\rho_{\text{ICM}}[r]/\rho_{\text{ICM}}[150\text{kpc}])^{2/3}$ assuming that the magnetic field is adiabatically compressed. We note that the spectra of particles (equations [9] and [10]) and synchrotron emission from high-energy electrons depend on B . Thus, the results shown below is fairly sensitive to the assumption on B .

In the following, the energy of an AGN explosion is $E_0 = 1.8 \times 10^{62}$ erg, which is three times larger than the one observed for MS 0735.6+7421 (McNamara et al. 2005). We use this value to match R_s with the size of the radio minihalo in the Perseus cluster. We take the acceleration efficiency of $\epsilon = 0.05$ to match radio observations (see below). The ratio of high-energy electrons to high-energy protons is taken to be $r_{e-p} = 1/1000$ as a fiducial value. In the self-similar solution of the shock we adopt, the kinetic and thermal energies are respectively constant. Therefore, we assume that the total energy of the high-energy protons is also constant. The typical Mach number of the shock in our calculations is ~ 3 (for $1 \times 10^7 < t < 4 \times 10^7$ yr). Performing simulations taking account of the back-reaction of accelerated particles on hydrodynamics, Ryu et al. (2003) estimated that the cosmic-ray acceleration efficiency is ~ 0.2 for that Mach number. Since they defined cosmic-ray as particles with energies larger than those of thermal particles (or the injection energy for acceleration), the fraction of protons having energies of $> m_p c^2$ must be smaller than 0.2.

Although it is not certain whether equation (4) can be extrapolated down to the injection energy, the adopted value of $\epsilon = 0.05$ is consistent with that of Ryu et al. (2003) because it is smaller than 0.2.

Fig. 1 shows the spectrum of nonthermal emission from accelerated particles at $t = 2 \times 10^7$ yr. The distance to the model cluster is 78.4 Mpc (the distance to the Perseus cluster¹). Synchrotron emission from primary electrons is dominant upto ~ 100 keV. The maximum energies for protons and electrons are $E_{\text{max,p}} = 6.8 \times 10^{17}$ eV and $E_{\text{max,e}} = 2.1 \times 10^{13}$ eV, respectively. The radius of the shock at this time is $R_s = 97$ kpc, the shock velocity is $V_s = 2650 \text{ km s}^{-1}$, and the Mach number is 2.7.

Fig. 2 shows the spectrum at $t = 4 \times 10^7$ yr. At this time, $E_{\text{max,p}} = 4.1 \times 10^{17}$ eV, $E_{\text{max,e}} = 2.1 \times 10^{13}$ eV, and $R_s = 143$ kpc, which is close to the size of the minihalo in the Perseus cluster. The shock velocity is $V_s = 1950 \text{ km s}^{-1}$ and the Mach number is 2.0. In Figs. 1 and 2, we plot the observed radio fluxes of the minihalo in the Perseus cluster (Sijbring 1993; Gitti et al. 2002). As can be seen, the predicted radio synchrotron emission (long-dashed line) is too bright to be consistent with the observations. If we take smaller E_0 , the radio luminosity becomes smaller. However, the size of the minihalo is too small to be consistent with the observed one. Moreover, if we consider a much smaller electron-proton ratio (e.g. $r_{e-p} \sim 10^{-5}$), the radio spectral index is inconsistent with the observations.

One possibility is that the age is much larger than 4×10^7 yr and is $t \gtrsim 10^8$ yr. At that time, the shock is not prominent because it is almost in pressure equilibrium with the surrounding ICM. In fact, for the Perseus cluster, a shock of $R_s \sim 100$ –200 kpc has not been reported. As the shock expands, its Mach number decreases from 2.7 (at $t = 2 \times 10^7$ yr) to 2.0 (at $t = 4 \times 10^7$ yr). Accordingly, the compression ratio (r_b) decreases, which affects the energy spectrum of particles and the emission from them (eq. [4]). Ryu et al. (2003) indicated that particles are no longer accelerated if the Mach number is $\lesssim 2$. Thus, for $t \gtrsim 4 \times 10^7$ yr, particle acceleration at the shock is not effective.

At $t \sim 10^8$ yr, the emission from primary electrons may have died out, because electrons with a Lorentz factor of $\gamma \gtrsim 10^4$, which are responsible for the radio emission, lose their energy through synchrotron emission and inverse Compton emission on a time-scale of $\lesssim 4 \times 10^7$ (e.g. Sarazin 1999). On the other hand, the lifetime of protons is much larger than 10^8 yr (eq. [7]), and the diffusion time of protons having the maximum energy of $\sim 10^{17}$ eV from the central region of the cluster (~ 200 kpc) is 2×10^8 yr (Völk, Aharonian, & Breitschwerdt 1996). Since particles are no longer accelerated at $t \gtrsim 4 \times 10^7$ yr, the overall spectrum

¹The redshift of the Perseus cluster is 0.0183. We assumed that the cosmological parameters are $\Omega_0 = 0.3$, $\lambda_0 = 0.7$, and $H_0 = 70 \text{ km s}^{-1} \text{ Mpc}^{-1}$

originated from proton-proton collisions stays almost intact for $4 \times 10^7 \lesssim t \lesssim 2 \times 10^8$ yr. In the radio band, only synchrotron emission from secondary electrons (dot-dashed line in Fig. 2) will be observed at $t \sim 10^8$ yr. In this case, the predicted spectrum (thick-solid line in Fig. 2) well fits the radio observations. Since the secondary radio emission is produced by protons having energies of ~ 100 GeV and since the diffusion time of these protons is $> \text{Gyr}$, the radio emission could persist that time. We emphasize that the assumption on the electron-proton ratio (r_{e-p}) is not required to estimate the emission originated from proton collisions.

4. Discussion

Although our model is basically an one-zone model and cannot quantitatively predict the spatial change of the spectrum, we can qualitatively predict that. Compared with the one at $t = 2 \times 10^7$ yr (Fig. 1), the spectrum of synchrotron emission from secondary electrons at $t = 4 \times 10^7$ yr is softer in the radio band ($\sim 0.3\text{--}1$ GHz; Fig. 2). The spectral index in the band of 327–609 MHz changes from 1.64 ($t = 2 \times 10^7$ yr, $R_s = 97$ kpc) to 1.88 ($t = 4 \times 10^7$ yr, $R_s = 142$ kpc). Since some of the protons accelerated at an earlier time should remain in the inner region of a cluster, the spectrum should be less steep in the inner region. This tendency is consistent with observations (Sijbring 1993; Gitti et al. 2002).

As we mentioned above, the radio emission from secondary electrons could persist for a long time ($> \text{Gyr}$). Our model will be tested for the frequency (or the event rate) of large outbursts. Gitti et al. (2007) indicated that large outbursts are likely occurring $\sim 10\%$ of the time in a significant proportion of all cooling core clusters. Thus, our model would suggest that a large fraction of clusters should have minihalos. This is inconsistent with the rareness of minihalos. However, the outbursts observed so far are of energies of $< 10^{62}$ erg (Rafferty et al. 2006), which is smaller than our finding (1.8×10^{62} erg). Thus, the rareness may indicate that strong AGN outbursts with energies of $> 10^{62}$ erg are rare phenomena or minor cluster mergers often perturb cluster cores. Another possibility is that particle acceleration at low-Mach number shocks occurs only in some specific IGM environments depending on the density of the surrounding matter, magnetic field configurations, and so on. In the future, statistical studies about AGN outbursts of $\sim 10^{62}$ erg are highly desired. The morphology of the radio surface brightness would also be important to check the validity of the model. If the particle acceleration is triggered by the expanding shock, one would expect a torus-like shape instead of the spherical shape observed for minihalos (Gitti et al. 2002). However, for clusters observed so far, the central region behind the shock is not empty; the ICM is still filling (e.g. Fig. 3 of McNamara et al. 2005). Thermal protons there

may work as target protons for the proton-proton interaction and thus the radio emission may not be a torus-like shape. A spatially resolved model must be constructed to address this issue.

In Figs. 1 and 2, we also plot the observational upper limits of gamma-ray emission from the Perseus cluster (Perkins et al. 2006). At $t = 2 \times 10^7$ yr, the gamma-ray emission is brighter than the observations. At $t \sim 10^8$ yr, there is no longer emission from primary electrons, and only gamma-ray emission of proton origin (thick-solid line in Fig. 2) will be observed in the gamma-ray band. The predicted gamma-ray flux at $E \sim 10^9$ eV is $\sim 1 \times 10^{-12}$ erg cm $^{-2}$ s $^{-1}$, which could be detected with *GLAST*² with a sensitivity of $\sim 3 \times 10^{-13}$ erg cm $^{-2}$ s $^{-1}$. The gamma-ray emission would persist for $\sim t_{pp}$. If the gamma-ray is detected, it directly indicates that protons as well as electrons are accelerated in clusters. Moreover, the luminosity reflects the total energy of the protons.

On the other hand, it would be difficult to detect the emission with imaging atmospheric Cherenkov telescopes. For example, *H.E.S.S.*³ has a sensitivity of $\sim 1 \times 10^{-13}$ erg cm $^{-2}$ s $^{-1}$ at $\sim 10^{12}$ eV). The predicted flux is smaller than the detection limit (Fig. 2).

The authors wish to thank the referee for useful comments. We are also grateful to T. Mizuno and Y. Ohira for fruitful discussions. Y. F. and R. Y. were each supported in part by Grants-in-Aid from the Ministry of Education, Science, Sports, and Culture of Japan (Y. F.: 17740162, R. Y.: 18740153). K. K. was also supported in part by NASA grant NNG04GL38G, PPARC grant, PP/D000394/1, EU grant MRTN-CT-2006-035863, the European Union through the Marie Curie Research and Training Network "UniverseNet" (MRTN-CT-2006-035863)

REFERENCES

- Atoyan, A. M., & Aharonian, F. A. 1999, MNRAS, 302, 253
- Baum, S. A., & O’Dea, C. P. 1991, MNRAS, 250, 737
- Blandford, R., & Eichler, D. 1987, Phys. Rep., 154, 1
- Brunetti, G., Blasi, P., Cassano, R., & Gabici, S. 2004, MNRAS, 350, 1174

²<http://www-glast.slac.stanford.edu/software/IS/glast%5Flat%5Fperformance.htm>

³<http://www.mpi-hd.mpg.de/hfm/HESS/HESS.html>

- Brunetti, G., Setti, G., Feretti, L., & Giovannini, G. 2001, MNRAS, 320, 365
- Burns, J. O., Sulkanen, M. E., Gisler, G. R., & Perley, R. A. 1992, ApJ, 388, L49
- Churazov, E., Forman, W., Jones, C., Böhringer, H. 2003, ApJ, 590, 225
- Clarke, T. E., Kronberg, P. P., Böhringer, H. 2001, ApJ, 547, L111
- Fujita, Y., & Sarazin, C. L. 2001, ApJ, 563, 660
- Fujita, Y., Takizawa, M., & Sarazin, C. L. 2003, ApJ, 584, 190
- Giovannini, G., & Feretti, L. 2000, New Astronomy, 5, 335
- Giovannini, G., Feretti, L., Venturi, T., Kim, K.-T., & Kronberg, P. P. 1993, ApJ, 406, 399
- Gitti, M., Brunetti, G., & Setti, G. 2002, A&A, 386, 456
- Gitti, M., McNamara, B. R., Nulsen, P. E. J., & Wise, M. W. 2007, ApJ, 660, 1118
- Hinton, J. A., & Domainko, W. 2007, submitted to MNRAS(astro-ph/0701033)
- Jokipii, J. R. 1987, ApJ, 313, 842
- Kempner, J. C., & Sarazin, C. L. 2001, ApJ, 548, 639
- Kim, K.-T., Kronberg, P. P., Dewdney, P. E., & Landecker, T. L. 1990, ApJ, 355, 29
- Kohri, K., Yamazaki, R., & Bamba, A. 2007 in preparation
- McNamara, B. R., Nulsen, P. E. J., Wise, M. W., Rafferty, D. A., Carilli, C., Sarazin, C. L., & Blanton, E. L. 2005, Nature, 433, 45
- Nulsen, P. E. J., Hambrick, D. C., McNamara, B. R., Rafferty, D., Birzan, L., Wise, M. W., & David, L. P. 2005a, ApJ, 625, L9
- Nulsen, P. E. J., McNamara, B. R., Wise, M. W., & David, L. P. 2005b, ApJ, 628, 629
- Ohno, H., Takizawa, M., & Shibata, S. 2002, ApJ, 577, 658
- Ostriker, J. P., & McKee, C. F. 1988, Reviews of Modern Physics, 60, 1
- Perkins, J. S., et al. 2006, ApJ, 644, 148
- Pfrommer, C., & Enßlin, T. A. 2004, A&A, 413, 17
- Rafferty, D. A., McNamara, B. R., Nulsen, P. E. J., & Wise, M. W. 2006, ApJ, 652, 216

- Rizza, E., Loken, C., Bliton, M., Roettiger, K., Burns, J. O., & Owen, F. N. 2000, *AJ*, 119, 21
- Roettiger, K., Burns, J. O., & Stone, J. M. 1999, *ApJ*, 518, 603
- Ryu, D., Kang, H., Hallman, E., & Jones, T. W. 2003, *ApJ*, 593, 599
- Sarazin, C. L. 1999, *ApJ*, 520, 529
- Sijbring, D. 1993, A Radio Continuum and HI Line Study of the Perseus Cluster, Ph.D. Thesis, Groningen
- Sturner, S. J., Skibo, J. G., Dermer, C. D., & Mattox, J. R. 1997, *ApJ*, 490, 619
- Takizawa, M., & Naito, T. 2000, *ApJ*, 535, 586
- Völk, H. J., Aharonian, F. A., & Breitschwerdt, D. 1996, *Space Science Reviews*, 75, 279
- Wise, M. W., McNamara, B. R., Nulsen, P. E. J., Houck, J. C., & David, L. P. 2007, *ApJ*, 659, 1153
- Yamazaki, R., Kohri, K., Bamba, A., Yoshida, T., Tsuribe, T., & Takahara, F. 2006, *MNRAS*, 371, 1975
- Yamazaki, R., Yoshida, T., Terasawa, T., Bamba, A., & Koyama, K. 2004, *A&A*, 416, 595

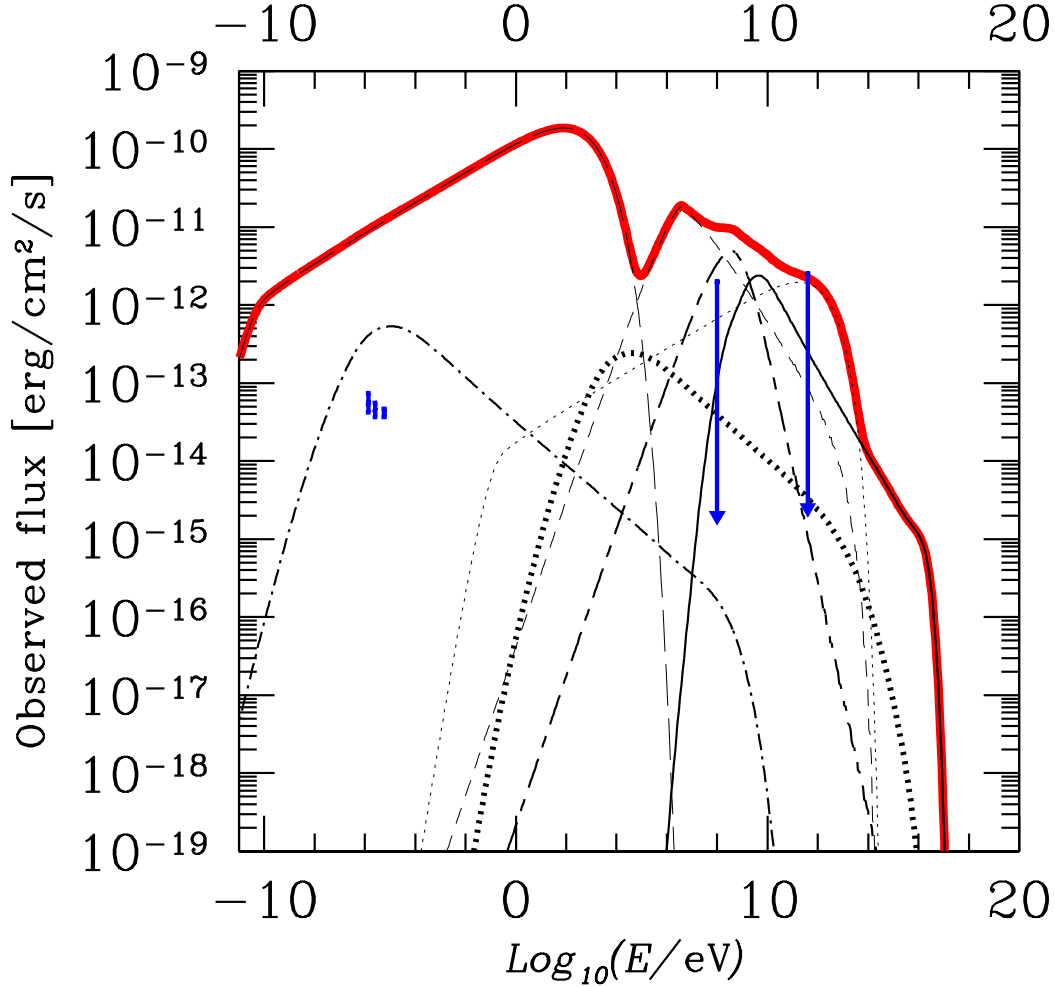


Fig. 1.— The spectrum of a shock at $t = 2 \times 10^7$ yr. Emissions from primary electrons are synchrotron (long-dashed), bremsstrahlung (short-dashed) and inverse Compton (thin dotted). Emissions related to protons are π^0 -decay gamma-ray (thin-solid), synchrotron (dot-dashed), bremsstrahlung (short-and-long dashed), and inverse Compton (thick-dotted) emissions from secondary electrons. The thick-solid line shows the total nonthermal flux. Radio observations are shown by dots (Sijbring 1993; Gitti et al. 2002), and gamma-ray upper limits are shown by arrows (Perkins et al. 2006).

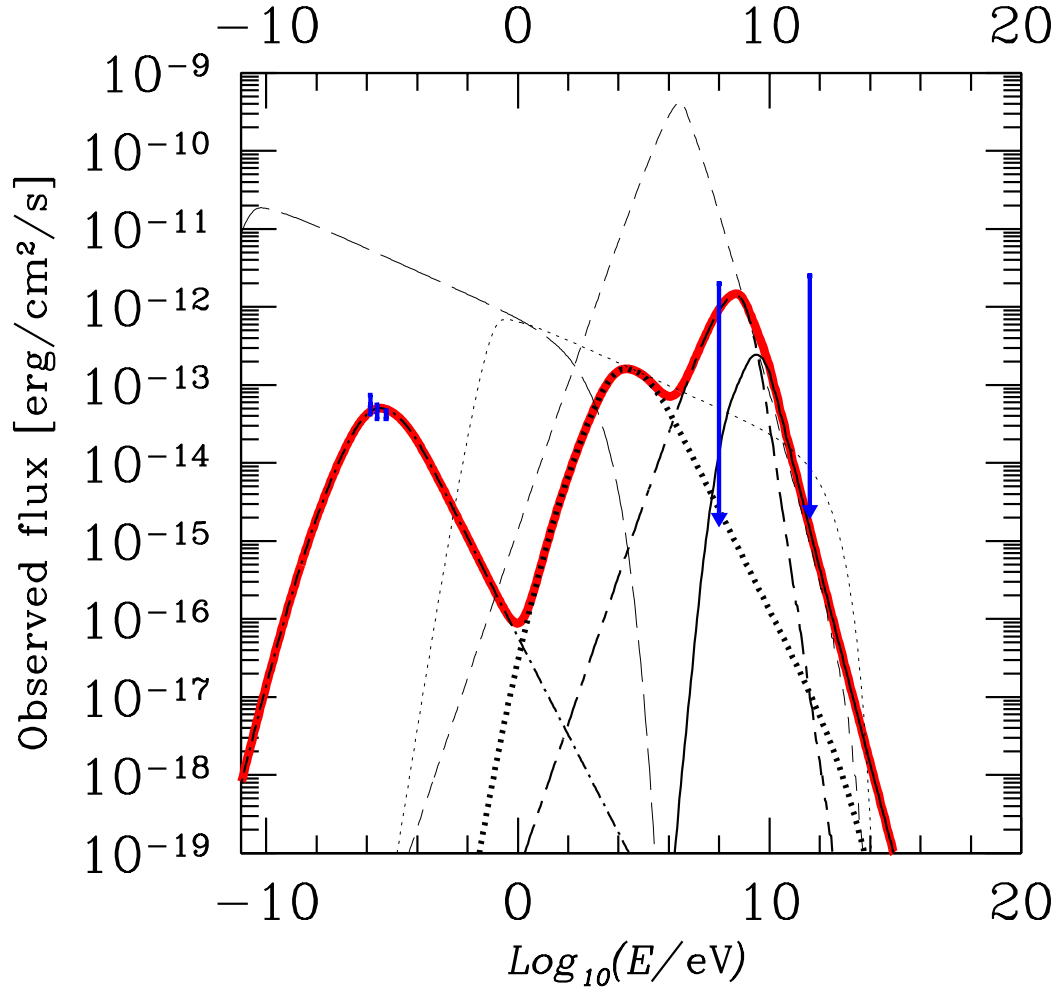


Fig. 2.— Same as Fig. 1, but for $t = 4 \times 10^7$ yr. In contrast with Fig. 1, the thick-solid line shows the flux from protons.